DEGRADATION OF REACTIVE ORANGE 16 USING A PROTOTYPE ATMOSPHERIC-PRESSURE NON-THERMAL PLASMA REACTOR [†]

UDC 533.92 : 547.556.33

Saša A. Rančev[1], Milica M. Petrović[2], Aleksandar Lj. Bojić[2], Dragan Đ. Radivojević[1], Čedomir A. Maluckov[3], Miodrag K. Radović[1]

[a]Department of Physics, Faculty of Sciences and Mathematics, University of Niš, Niš, Serbia
[b]Department of Chemistry, Faculty of Sciences and Mathematics, University of Niš, Niš, Serbia
[c]Department for inorganic chemical technology, Technical Faculty in Bor, University of Belgrade, Bor, Serbia

Abstract. *A prototype atmospheric pressure non-thermal corona plasma reactor system is developed and tested for the removal of commercial textile reactive dye from water. The dye can be completely degraded in water by the presented reactor system in the initial concentration range of 10-100 mg dm^{-3}. Dye degradation rate decreases with the increase of initial dye concentration and pulse frequency. The pH of treated solutions decreases with the increase of treatment time and with the decrease of the applied frequency. Solutions electrical conductivity increases with an increase of treatment time and with the decrease of the applied frequency. The decolorization reactions follow the pseudo-first kinetics order. The changes in the treated dye solutions compositions are the consequences of injection of plasma generated reactive species from gas into the liquid through the interfacial zone.*

Key words: *plasma, air, dye, degradation, pH, conductivity*

1. INTRODUCTION

The interaction of non-equilibrium plasmas with a liquid state is applied in many areas including environmental applications, especially in the wastewater treatments (Bruggeman and Leys, 2009).

Synthetic organic dyes are very stable and resistant to light, heat, common oxidizing agents and aerobic biological degradation, which makes them very difficult to remove from wastewater by the conventional treatments (e.g. Sun and Yang, 2003). The Advanced Oxidation Processes (AOPs) are, however, capable to degrade dyes molecules by oxidation via highly reactive, short-living oxygen species with very high oxidative potential, like hydroxyl radical, •OH ($E^0 = 2.80$ V).

These processes, in which •OH radicals are generated, involve electrochemical oxidation (e.g. Martı́nez-Huitle and Brillas, 2009), UV radiation in the presence of O_3, H_2O_2, photocatalyst, etc. (e.g. Simonenko et al., 2015) and various types of plasmas, such as pulsed corona discharge, dielectric-barrier discharge, atmospheric non-thermal plasma torch and jet, as well as atmospheric pressure non-thermal plasma corona (Magureanu et al., 2008; Tichonovasa et al., 2013; Bansode, et al, 2017; Chandana et al., 2015).

The plasma generated at air-water interface is a source of strong oxidants, like reactive ion and radical species, electrons, UV radiation, electric field etc. Some of them, such as aforementioned •OH radical, are capable of degrading various organics in a water medium.

In this paper, a prototype atmospheric pressure non-thermal corona plasma reactor system and its ability to remove a commercial textile dye Reactive Orange 16 (RO 16) from the water solution is described. The discharge was created in the gas phase using multipin electrode over a liquid, which was used as an anode. The liquid itself was a cathode.

Corona occurred in the strong non-uniformed electric field, on the spikes (conductors with a small radius of curvature), and is characterized with low current intensity and a correspondingly small level of emitted light (e.g. Raizer, 1991).

2. Experimental

2.1. Equipment

A multipin-water electrode geometry was used to generate corona in the air at atmospheric pressure. The experimental set-up (Figure 1) consists of a plasma DC pulse generator and reactor chamber which were developed and tested in our Research Laboratory for Gas Discharges. The corona discharge was created near the multipoint anode, composed of stainless steel needles in the gas phase above the liquid. The electrode contains 97 needles and their mutual distance was 2.5 mm. They were soldered on the circular printed circuit board (PCB), with a diameter of 29 mm, all at the same potential. The surface of the conductive liquid acts as a cathode for this discharge and surface area of the liquid electrode is 16.61 cm^2. The reactor cell is made of polyvinyl chloride (PVC) in a cylindrical shape. The HV ratios and the frequency (in the range from 10 to 100 kHz) of the pulses were controlled. The distance (d) from the anode to the liquid surface was 16 mm in these experiments. The electrical current of discharge was measured by the multimeter Iskra Unimer 06. The discharge current density was calculated based on the measured discharge current values and the surface of the liquid electrode, and it was 9.15 μA/cm^2. The volume of the samples was 10 cm^3.
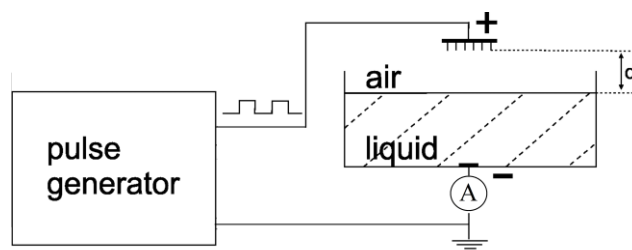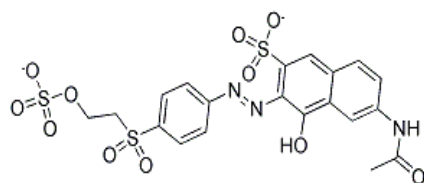
Fig. 1. Schematic of the experimental set-up

2.2. Materials and Methods

RO 16 was obtained from Farbotex (Italy) and used without further purification. All solutions were prepared in deionized water (18.2 MΩ, Smart2Pure, Thermo Scientific, USA).

Table 1. The main characteristics of RO 16

Dye	Chemical structure		Molar mass (g mol^{-1})	Λ_{max} (nm)
Reactive Orange 16	Na$^+$	Na$^+$	617.54	493

2.3. Experimental Procedure

Dye decolorization experiments were carried out at an ambient temperature of 20±0.5 °C (which was held constant during the experiments, at various initial dye concentrations. RO 16 solutions of 10.0, 20.0, 50.0, 80.0 and 100.0 mg dm^{-3} were prepared separately by dissolving 1000.0 mg of a powdered dye in 1 dm^{-3} of water (stock solution) and further diluting required amounts of stock solution to obtain the required concentration dye solutions. The samples of the solutions were taken at the certain time intervals and measured by UV-VIS spectrophotometer Shimadzu UV-1650 PC (Shimadzu, Japan). The percentage of decolorization was calculated using the equation:

$$\text{Percentage of decoloriza tion (\%)} = \frac{C_0 - C}{C_0} \times 100 \tag{2.1}$$

Where C_0 is the initial dye concentration and C is the dye concentration at the time t. All the experiments were done starting at the solutions initial native pH and conductivity.

Electrical conductivity and pH of the solutions were measured during the treatment using pH meter (SensIon3, Hach, USA) and conductometer (SensIon5). All experiments were conducted in triplicate and gave reproducibility of within 2%.
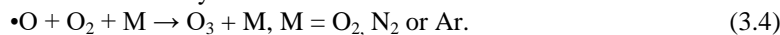
3. RESULTS AND DISCUSSION

3.1. Plasma chemistry

Fast electrons produced in the non-thermal plasma can have energies of the order 10 eV. The primary source of all reactions is electron impact on the bulk gas molecules. It produces many reactive species as radicals: •OH, •O, and •NO; excited N_2 molecules; and atomic and molecular ions (e.g. O^+, O_2^+), which can react further with more stable species (e.g. Nijdam et al, 2012).

Producing of free oxygen radicals by inelastic electron impact on molecules in air:

$$O_2 + e \rightarrow O^+ + \bullet O + 2e \tag{3.1}$$
$$O_2 + e \rightarrow O + \bullet O + e \tag{3.2}$$
$$O_2 + e \rightarrow O^- + \bullet O \tag{3.3}$$
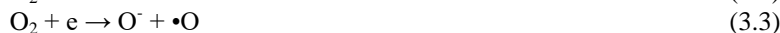
After that the ozone is created by

$$\bullet O + O_2 + M \rightarrow O_3 + M, \ M = O_2, \ N_2 \ \text{or Ar.} \tag{3.4}$$

Formation of NO_x in the air can be presented in the following way (e.g. Lewis et al., 2003; e.g. Bruggeman et al., 2016):

$$N + O_2 \rightarrow NO + \bullet O \tag{3.5}$$
$$\bullet O + N_2 \rightarrow NO + N \tag{3.6}$$
$$N_2 + O_2 + e \rightarrow 2NO + e \tag{3.7}$$

The N_2 molecule can be dissociated by electron impact:

$$N_2 + e \rightarrow N + N + e \tag{3.8}$$

Furthermore, the produced NO can react with O_2 (e.g. Bruggeman et al., 2008); e.g. Bruggeman et al., 2008a)

$$\bullet O + NO + M \rightarrow NO_2 + M \tag{3.9}$$
$$2NO + O_2 \rightarrow 2NO_2 \tag{3.10}$$
$$2NO + O_2 \rightarrow NO_2 + N + O_2 \tag{3.11}$$

The removal of NO from the air at low NO concentrations is represented by the Eq. (3.8) followed with the reaction (3.12) (e.g. Bruggeman et al., 2007)

$$N + NO \rightarrow N_2 + \bullet O \tag{3.12}$$

A second important radical is •OH. It is produced in moist gases (e.g., moist air) by the following reaction (e.g. Bruggeman et al., 2008b)
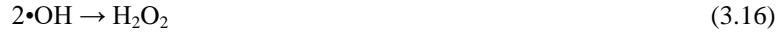
$$H_2O + e \rightarrow H + \bullet OH + e \tag{3.13}$$

Formation of acids HNO_2, HNO_3 is represented by the following reactions (e.g. Bruggeman et al., 2016):

$$NO + \bullet OH \rightarrow HNO_2 \tag{3.14}$$
$$NO_2 + \bullet OH \rightarrow HNO_3 \tag{3.15}$$
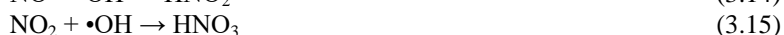
In the plasma-liquid interactions, chemical reactions most likely occur in the bulk liquid and the gas phase. At the gas-liquid interface, they appear simultaneously with transport processes.

The reaction

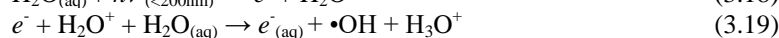$$2 \cdot OH \rightarrow H_2O_2 \qquad\qquad (3.16)$$

represents the formation of hydrogen peroxide by hydroxyl radical recombination. It can appear in the gas (g), the liquid (aq) or at the gas-liquid interface
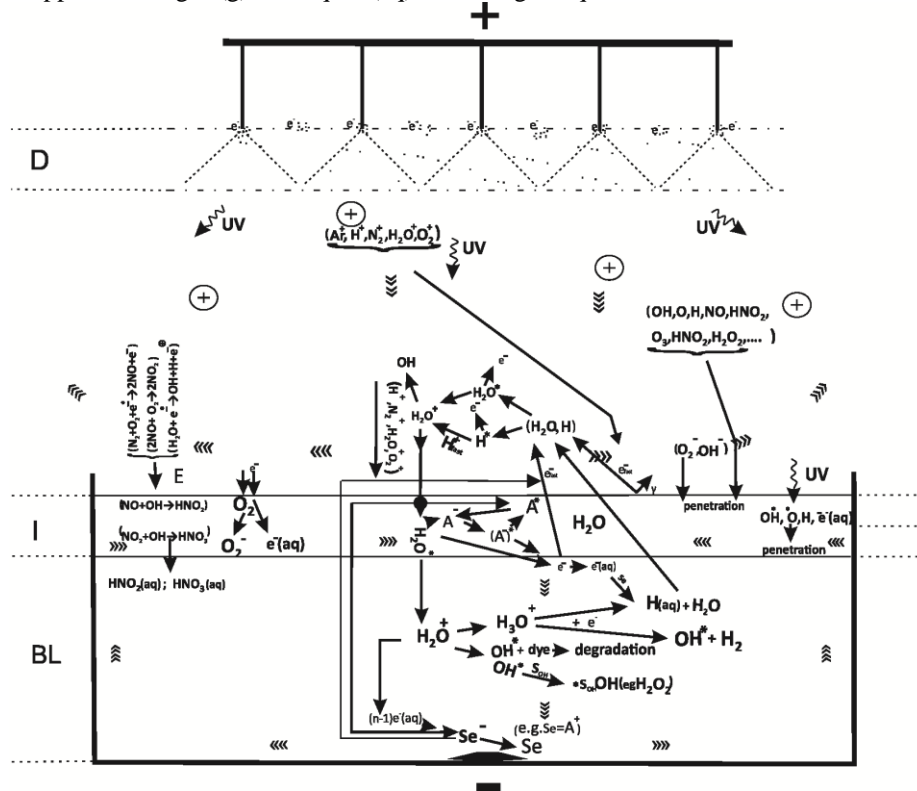
Fig. 2. Schematic diagram of plasma chemical processes. Positive ions and UV photons are produced in the discharge zone (D); I - interfacial zone; BL - bulk liquid. Circulations in air and liquid are indicated by multiple arrows.

Corona discharge over the water surface, with a gas gap containing air, can also produce nitrates and nitrites. NO and NO_2 are formed in the gas phase from the nitrogen in the air. These products further react with water, hydroxyl radicals and other oxidants in the liquid phase. That way, nitrate, and nitrite are formed, which induce pH changes in the liquid phase (e.g. Locke at al. 2006).

Air plasma discharges also emit UV radiation which is an important process of the plasma produced chemistry in liquid. When UV radiation is absorbed in the liquid water with dissolved gases such as O_2, the most important reactions are (e.g. Bruggeman and Leys, 2009):

$$H_2O_{(aq)} + h\nu \rightarrow \bullet OH + \bullet H \qquad (3.17)$$

$$H_2O_{(aq)} + h\nu_{(<200nm)} \rightarrow e^- + H_2O^+ \qquad (3.18)$$

$$e^- + H_2O^+ + H_2O_{(aq)} \rightarrow e^-_{(aq)} + \bullet OH + H_3O^+ \qquad (3.19)$$

$$H_2O(g) + h\nu \rightarrow \bullet OH + \bullet H \qquad (3.20)$$

$$H_2O(g) + h\nu \rightarrow H_2 + \bullet O(1D) \qquad (3.21)$$

$$O_2 + h\nu \rightarrow 2\bullet O \qquad (3.22)$$

As can be seen, plasma-induced UV radiation also contributes to a formation of •OH radicals.

3.2. Effect of Initial Dye Concentration and Decolorization Kinetics

RB 19 shows high resistance to UV radiation alone and H_2O_2 in dark and light (e.g. Mitrović et al., 2012). When RO 16 water solution is exposed to air plasma, being practically a liquid cathode, a fast decolorization is observed. Dye was completely decolorized, in the tested range of initial concentrations. Dye removal efficiency decreases with the increase of its initial concentration, probably because of the higher number or reactant molecules. After the first ten minutes of the treatment, the decolorization efficiency, expressed as a % of the color removed, was 100%, 96.76%, 94.37%, 91.52%, and 84.81%, for the solutions of 10.0, 20.0, 50.0, 80.0 and 100.0 mg dm^{-3} initial dye concentration, respectively. Total decolorization time varies from about 10 minutes for the lower concentrations to little less than 25 minutes for the highest initial concentration.

Plasma decolorization of RO 16 approximately follows the pseudo-first-order kinetic model, which is described by the equation:

$$\ln(C/C_0) = -kt \qquad (3.28)$$

where C_0 is initial dye concentration, c is a dye concentration after reaction time t, and k is the reaction rate constant (min^{-1}). The plot of $\ln(C/C_0)$ against time scale for the plasma decolorization of RO 16 for a series of the initial dye concentrations ranging from 10 to 100 mg dm^{-3} (Figure 3) approximately shows a linear decrease with increasing reaction time.
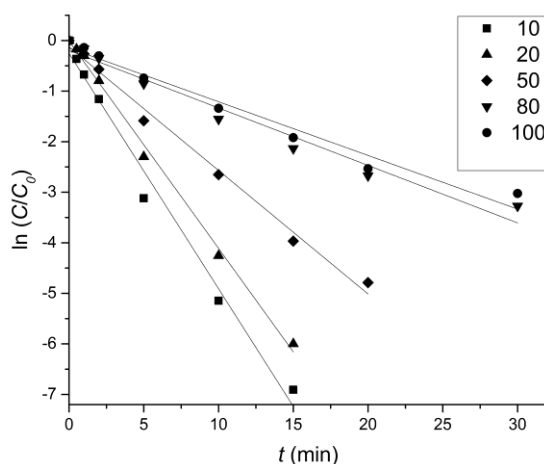
Fig. 3. Pseudo-first order kinetics model for plasma decolorization
of RO 16, C_0 is given in mg dm^{-3}

This is confirmed by the relatively high coefficient of determination (R^2) values of about 0.98-0.99 in the whole range of tested concentrations (Table 2) and is in accordance with the literature, which reports the pseudo-first-order kinetics reaction of organics by various AOPs, including certain types of plasmas (e.g. Chandana et al., 2015; e.g. Chandana and Subrahmanyam, 2016; e.g. Jiang et al., 2012; e.g. Petrović et al., 2015; e.g. Simonenko et al., 2015). These findings strongly indicate that the dye was degraded by the action of highly reactive oxygen species originating from the air plasma, generated in gas and gas-water interface and dissolved in water, eventually leading to a generation of •OH radicals, which oxidized and degraded dye molecule through mechanisms and reactions given above and elsewhere in literature (e.g. Bruggeman and Leys, 2009; e.g. Bruggeman et al., 2016; e.g. Barthakur, 1990)

Reaction rate constants decrease with the increase of initial dye concentration (Table 2), falling from 0.421 for the lowest to 0.23 for the highest initial concentration, most likely because the ratio between the amount of "*in situ*" produced •OH radicals and the remaining dye molecules becomes less favorable at the highest dyes concentration.

**Table 2.** Reaction rate constants and R^2 values for decolorization of RO 16

| C_0 (mg dm^{-3})	Reaction rate constant (min^{-1})	R^2
10	0.421	0.9914
20	0.351	0.9906
50	0.338	0.9823
80	0.302	0.9830
100	0.230	0.9825

3.2.1. The pH and conductivity of the plasma-treated dye solutions

Solutions pH decreases during the treatment, starting from its beginning (native) value (which varies from 5.27 to 5.01 for the initial dye concentration of 10 to 100 mg dm^{-3}, respectively) in a very similar manner for all the initial dye concentrations (Figure 4), no matter what their initial pH was. After 10 minutes of treatment, pH falls to about 2.9 for all the treated solution. A decrease of pH was also observed in other plasma treatments of organics in the aqueous medium (e.g. Chandana et al., 2015). Decrease of pH is explained by excitation of O_2 and N_2 molecules in air, their transformation to NO and NO_2 molecules via the mechanisms described in the section 3.1 and their further dissolution in water phase, leading to a generation of HNO_2 and HNO_3, which acidify the solutions (e.g. Chandana et al., 2015; e.g. Shang et al., 2017; e.g. Hentita et al., 2014).

An increase of the solution electrical conductivity (k) with the increase of treatment time is also observed (Figure 5). Electrical conductivity increases from 11.1 to 77.4 μS cm^{-1} for the initial dye concentration of 10 to 100 mg dm^{-3}, respectively and it originates from the presence of the dye molecules in water. As the treatment proceeds, conductivity increases for all the treated dye solutions, always being little higher at a certain treatment time for the solutions with the higher initial dye concentration. For the lower initial concentrations, k remains very similar during all the treatment for the same treatment time, but their corresponding k values are significantly different from those of the higher initial concentrations solutions at a certain time of treatment because the organic molecules contribute to the overall conductivity of the solutions.
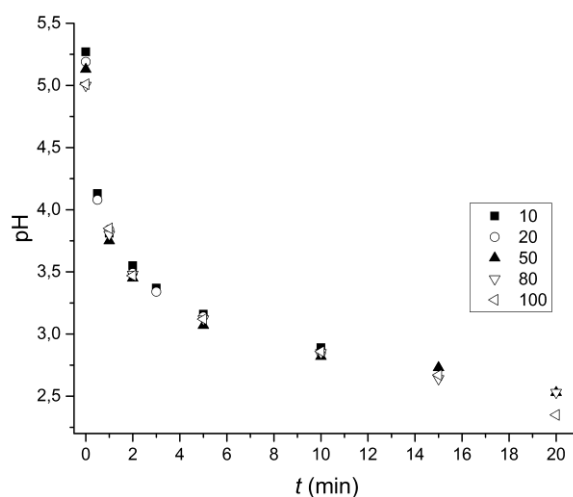
Fig. 4. Changes of pH during the plasma treatment of RO 16
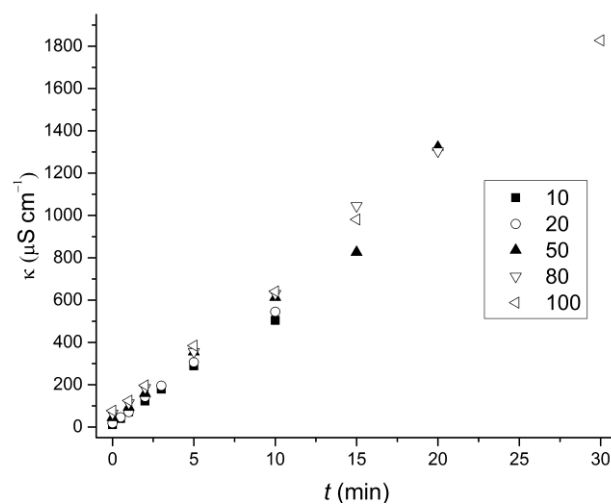
Fig. 5. Changes of electrical conductivity during the plasma treatment of RO 16

However, k increases in the same manner for all the dye solutions and the reason is generally the same as that for the decrease of pH: generation of nitrates and nitrites in dye water solution during the treatment. A very similar result regarding the increase of conductivity was obtained for the treatment of Crystal Violet dissolved in distilled water by DBD induced non-thermal plasma (e.g. Chen et al., 2017) and for the degradation of Methylene Blue dissolved in deionized water by the microwave atmospheric pressure plasma jet (e.g. García et al., 2017). Thus, during the plasma treatment of water medium, if N_2 is present in the gas phase, nitrogen radicals will also be generated and corresponding nitrogen species will be dissolved in the

water phase, along with the oxygen radicals. The concentration of both kinds increases during the treatment time.

3.3 Effect of frequency on the decolorization rate, pH and electrical conductivity

The 50 mg dm^{-3} dye water solutions were treated at various pulse frequencies (v) during the same time. The solutions were treated in the frequency range in which is possible to obtain a stable corona; the lowest frequency is the one where corona is still stable, just before it becomes unstable, creating sparks and conductive "plasma channels" in gas phase and the highest frequency is the one when corona becomes the weakest and disappears. As shown in Figure 6, dye decolorization efficiency decreases with the increase of v, from 68% at 10 kHz to only 26% at 50 kHz for the treatment time of 5 minutes.
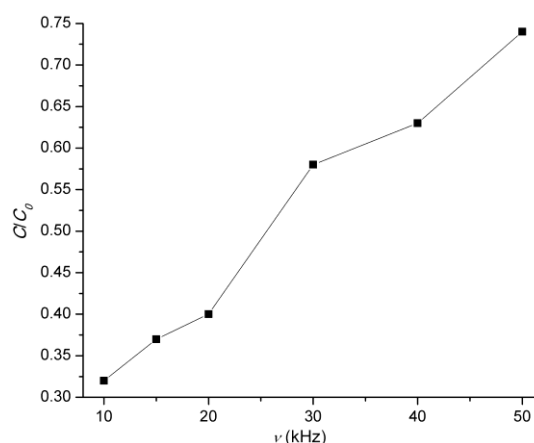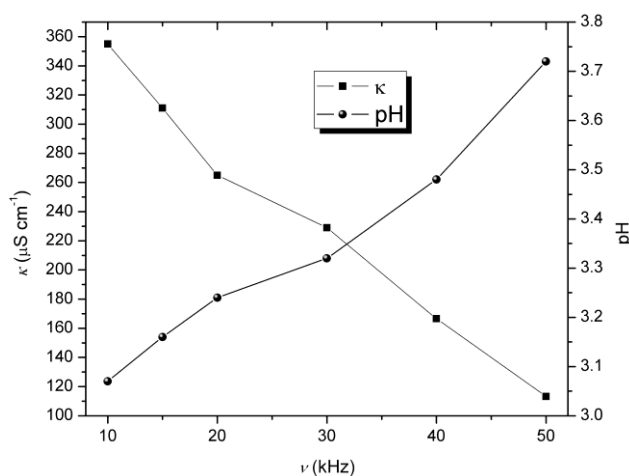

Fig. 6. Effect of applied frequency on dye degradation (C_0 (RO 16) =50 mg dm^{-3}, t = 5 min).

As discussed before, dye degradation is directly connected with the production of •OH radicals, which indicates that •OH generation in liquid is more intense at lower frequencies, probably because at the higher frequencies the pulses are not long enough to accelerate the generated electrons which strike the air constituents, creating radicals; at lower frequencies, the regime is closer to DC, which means that electrons have more time between impulses to accelerate and strike with higher kinetic energy, or have more successive collisions. The pH of the treated solutions is the lowest at 10 kHz (3.07) and it starts to significantly increase with the increase of frequency, reaching its maximum of 3.72 at 50 kHz. Having in mind that the pH reflects the concentration of HNO_2 and HNO_3 in solutions, which originate from the plasma nitrogen radicals, the results indicate that the production of nitrogen radicals becomes less intense as the treatment frequency increases, probably due to the same reason as for the oxygen radicals, including longer pauses between the pulses on lower frequencies when recombinations and forming of NO and NO_2 may be more probable.

Solution conductivity decreases with the increase of treatment frequency (Figure 7) basically reflecting the same phenomenon as pH, confirming the decrease of generation of nitrogen species in liquid with an increase in frequency. Overall, it can be assumed that

with the increase of treatment frequency the generation of both •OH radicals and nitrogen species in the liquid decreases.

Fig. 7 Effect of applied frequency on solutions pH
and electrical conductivity (C_0 (RO 16) =50 mg dm^{-3}, t = 5 min).

4. CONCLUSIONS

A prototype atmospheric pressure non-thermal corona plasma reactor system was successfully applied for the degradation of a commercial reactive textile dye from water. The dye was completely degraded in the tested concentrations range. Dye removal efficiency increases with the increase of treatment time and its removal rate decreases with the increase of initial dye concentration. It proceeds via oxidation of plasma-generated active oxygen species dissolved in liquid, following the pseudo-first kinetics order. Dye solutions pH decreases and their conductivity increases with the increase of reaction time due to the generation of HNO_2 and HNO_3 caused by dissolution of plasma-generated active nitrogen species. Dye degradation efficiency and solutions electrical conductivity decreases and the pH increases with the increase of treatment frequency, meaning that generation of both active oxygen and nitrogen species in liquid decrease when the treatment frequency increases.

REFERENCES

Bansode, A., More, S.E., Siddiqui, E., A., Satpute, S., Ahmad, A., Bhoraskar, S.V., Mathe, V., L., 2017, Chemosphere 167, 396-405, DOI:10.1016/j.chemosphere.2016.09.089
Barthakur, N., 1990. Desalanisation, 78, 455-465.
Bobkova, E., Smirnov, S., Zalipaeva, Y., Rybkin, V., 2014. Plasma Chem. Plasma Process, 34, 721-743.
Bruggeman et al., 2016. Plasma Sources Sci. Technol, 25, 053002. doi:10.1088/0963-0252/25/5/053002
Bruggeman P., Van Slycken, J., Degroote, J., Vierendeels, J., Verleysen, P., Leys, C., 2008. Plasma Sci. 36, 1138-1139.
Bruggeman, P., Graham, L., Degroote, J., Vierendeels, J., Leys, C., 2007. J. Phys. D: Appl. Phys. 40, 4779-4786.
Bruggeman, P., Guns, P., Degroote, J., Vierendeels, J., Leys, C., 2008. Plasma Sources Sci. Technol. 17, 045014.

Bruggeman, P., Leys, C., 2009, J. Phys. D: Appl. Phys. 42, 053001 1-28 doi:10.1088/0022-3727/42/5/053001

Bruggeman, P., Ribezl, E., Degroote, J., Vierendeels, J., Leys, C., 2008b. J. Optoelectron. Adv. Mater. 10, 1964–7. 000257962500014

Bugaenko, V., Byakov, V., 1998. High Energy Chem, 365-371.

Chandana, L., Manoj, P., Kumar, R., Subrahmanyam, C., 2015, Chem. Eng. J. 282, 116-122. doi.org/10.1016/j.cej.2015.02.027

Chandana, L., Subrahmanyam, Ch., 2016. J. Env. Chem. Eng., doi.org/10.1016/j.jece.2016.11.014,

Chen, J., Du, Y., Shen, Z., Lu, S., Su, K., Yuan, S., Hu, Z,. Zhang, A., Feng, J., 2017. Sep. Purif. Technol. 179, 135-144.

García, M., Mor, M., Esquivel, D., Foster, J., Rodero, J., Jimenez-Sanchidri, E., Romero-Salguero, F., 2017. Chemosphere, 180, 239-246. doi.org/10.1016/j.chemosphere.2017.03.126

Hentita, H., Ghezzarb, M., Womesc, M., Jumas, J., Addou, A., Ouali, M., 2014. J. Mol.Catal. A: Chem, 390, 37-44. doi.org/10.1016/j.molcata.2014.03.003

Jablonowski, H., Bussiahn, R., Hammer, M., Weltmann, D., von Woedtke, T., Reuter, S., 2014. Phys. Plasmas, 22, 122008.

Jiang, B., Zheng, J., Liu, Q., Wu, M., 2012. Chem. Eng. J, 204, 32-39, doi.org/10.1016/j.cej.2012.07.088

Lewis, T., 2003. Trans. Dielectr. Electr. Insul. 10, 948-955.

Locke, B., Sato, M., Sunka, P, Hoffmann, M., 2006. Eng. Chem. Res. 45, 882-905 DOI: 10.1021/ie050981u

Magureanu M., Piroi D., Gherendi, F., Mandache, N., Parvulescu, V., 2008. Plasma Chem. Plasma Process, 28, -688.

Martı´nez-Huitle, C.A., Brillas, E., 2009. Appl. Catal. B, 87, 105-145, doi:10.1016/j.apcatb.2008.09.017

Mitrović, J., Radović, M., Bojić, D., Anđelković, T., Purenović, M., Bojić, A., 2012. J. Serb. Chem. Soc. 77, 465-481. doi: 10.2298/JSC110216187M

Nijdam, S., Van Veldhuizen, E., Bruggeman, P., Ebert U., 2012. An introduction to nonequilibrium plasmas at atmospheric temperature in: V.I. Parvulescu, M. Magureanu, P. Lukes (Eds.), Plasma Chemistry and Catalysis in Gases and Liquids, Wiley, NY, 1-44.

Petrović, M., Mitrović, J., Antonijević, M., Matović, B., Bojić, D., Bojić, A., 2015, Mat. Chem. Phys, 158, 31-37, doi.org/10.1016/j.matchemphys.2015.03.030

Raizer, Y.,1991. Gas Discharge Physics, Springer, Berlin.

Shang, K., Wan, X., Li, J., Wang, H., Lu, N., Jiang, N., Wu, Y., 2017. Chem. Eng. J. 311, 378-384. doi.org/10.1016/j.seppur.2017.02.007

Simonenko, E., Gomonov, A., Rolle, N., Molodkina, L., 2015. Procedia Engineering, 117, 337-344. doi.org/10.1016/j.proeng.2015.08.170

Sun, Q., Yang, L., 2003. Water Res. 37, 1535-1544, DOI: 10.1016/S0043-1354(02)00520-1

Tichonovasa, M., Krugly, E., Racys, V., Hippler, R., Kauneliene, V., Stasiulaitiene, I., Martuzevicius, D., 2013, Chem. Eng. J. 229, 9-19.

DEGRADACIJA REAKTIVNE NARANDŽASTE BOJE RO16 KORIŠĆENJEM PROTOTIPA KORONA REAKTORA SA HLADNOM PLAZMOM NA ATMOSFERSKOM PRITISKU

Prototip atmosferskog korona reaktora sa hladnom plazmom razvijen je i testiran za razgradnju komercijalne reaktivne tekstilne boje u vodi. Boja može biti potpuno razgrađena primenom navedenog plazma reaktora u opsegu početnih koncentracija od 10-100 mg dm^{-3}. Brzina razgradnje boje opada sa porastom početne koncentracije i povećanjem primenjene frekvence impulsa. Vrednost pH tretiranih rastvora opada sa porastom vremena tretmana i smanjenjem primenjene frekvence. Električna provodnost rastvora raste sa porastom vremena tretmana i sa smanjenjem primenjene frekvence. Reakcije obezbojavanja slede kinetiku pseudo-prvog reda. Promene u sastavu tretiranih rastvora su posledica prelaska plazma-generisanih reaktivnih vrsta iz gasa u tečnost kroz granični sloj.

Ključne reči: *plazma, vazduh, boja, degradacija, pH, provodljivost*